Observation of Optically Induced Feshbach Resonances in Collisions of Cold Atoms

F. K. Fatemi,[1] K. M. Jones,[2] and P. D. Lett[1]

[1]*Atomic Physics Division, National Institute of Standards and Technology, Gaithersburg, Maryland 20899-8424*
[2]*Physics Department, Williams College, Willamstown, Massachusetts 01267*

(Received 6 June 2000)

We have observed optically induced Feshbach resonances in a cold (<1 mK) sodium vapor. The optical coupling of the ground and excited-state potentials changes the scattering properties of an ultracold gas in much the same way as recently observed magnetically induced Feshbach resonances, but allows for some experimental conveniences associated with using lasers. The scattering properties can be varied by changing either the intensity or the detuning of a laser tuned near a photoassociation transition to a molecular state in the dimer. In principle this method allows the scattering length of any atomic species to be altered. A simple model is used to fit the dispersive resonance line shapes.

PACS numbers: 32.80.Pj, 34.20.Cf, 34.50.Rk, 34.80.Qb

A Feshbach resonance in a scattering process occurs when a bound state in a normally inaccessible potential (closed channel) is located at the energy of the incoming scattering flux. Some of the flux can then tunnel and couple into and out of this quasibound state, where it can build up and alter the phase of the reflected wave function. In the extremely low-energy collisions typical in laser cooling experiments such a resonance is achieved by having this quasibound state at or near zero energy. This changes the scattering properties which are essential to the achievement and description of a Bose-Einstein condensate (BEC). One way to produce a Feshbach resonance is by using a magnetic field to mix ground state potentials that connect to different hyperfine asymptotes. A bound state of one potential is Zeeman shifted into resonance with the incoming flux on another hyperfine potential. Such magnetically induced Feshbach resonances have been used to alter scattering and condensate properties [1–5], and have even permitted the condensation of a new species [6].

Alternative means of inducing Feshbach resonances may have experimental advantages. The uses of rf [7] and dc electric fields [8] have been suggested. Fedichev *et al.* [9] first suggested using optical fields and this concept has been further investigated theoretically in [10,11]. The ease and rapidity with which both the intensity and detuning of laser fields can be manipulated and the ability to spatially localize a change in the scattering length make this an appealing alternative to magnetic fields in some situations. Optical transitions are always available, even when hyperfine structure is absent, such as in the most common isotopes of the alkaline earth elements. In this work we report the observation and characterization of such optically induced Feshbach resonances in a cold sodium vapor.

We use the technique of photoassociation spectroscopy [2,12], where colliding atoms absorb a photon and produce a bound, excited molecule, both to induce and observe the Feshbach resonance. We create a coupling to an excited molecular potential whenever a laser is tuned near a photoassociation transition. A strong coupling can be viewed as a Feshbach resonance in a dressed-state picture.

We first construct a monitor for the behavior of the ground state wave function. A weak laser (L_1) is introduced into a cold gas held in a magneto-optical trap (MOT) and is tuned to a photoassociation (PA) transition to create the excited molecular state $|e1\rangle$. Photons from a second laser (L_{ion}) promote these molecules to an autoionizing doubly excited state, producing Na_2^+ ions which are collected and counted (see Fig. 1a). These lasers are fixed in tuning and intensity, and produce a constant ion signal which is proportional to the photoassociation rate. This rate is determined by the density of colliding atoms with separations approximately equal to the Condon radius R_C, where the photon energy matches the difference between the potentials. A third, strong laser (L_2) is introduced and scanned through $|e2\rangle$, producing changes in the ion signal. Strong dispersive signals, such as those in Fig. 2, are obtained due to the creation of optical Feshbach resonances.

There are several other processes by which L_2 can produce changes in the ion signal. For example, the scanning laser might drive molecules out of the intermediate

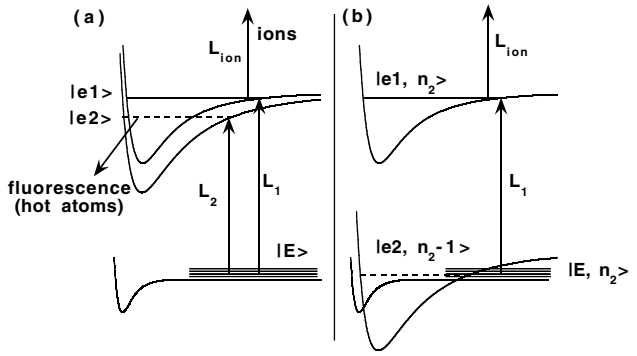

FIG. 1. Sketch of the lasers, energy levels, and potential surfaces involved in observing an optically induced Feshbach resonance in (a) the undressed picture, and (b) the dressed-state picture. The states are dressed with the number of photons in the field of laser 2; as the detuning of L_2 is changed from red to blue the resonance is scanned downward through zero collision energy.

 0031-9007/00/85(21)/4462(4)$15.00

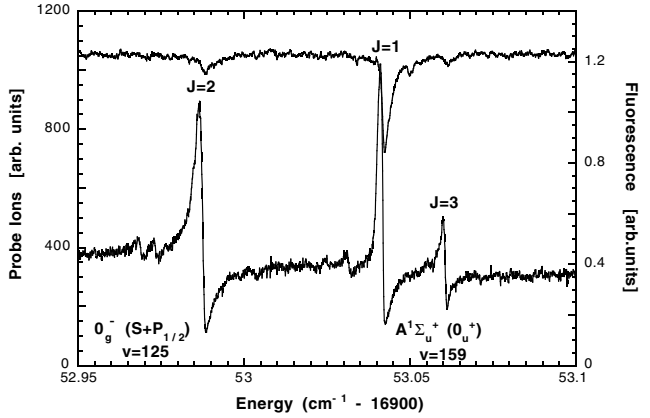

FIG. 2. Ion signal (lower) and trap loss (upper) as functions of the detuning of laser 2. The laser intensities are fixed at L_1: 4 W/cm^2; L_{ion}: 10 W/cm^2; L_2: 100 W/cm^2. Laser 1 is fixed on the $0_g^-(S + P_{1/2})$ $v = 123$, $J = 2$ resonance. Resonances identified in the scan are to the $0_g^-(S + P_{1/2})$ $v = 125$, $J = 2$ level and the $A^1\Sigma_u^+(0_u^+)$ $v = 159$, $J = 1, 3$ levels.

state $|e1\rangle$, down to high levels in the collision continuum, thereby reducing the ionization signal [12]. Alternatively, it can excite molecules from $|e1\rangle$ up to doubly excited levels which may or may not be autoionizing, thus producing an increase or a decrease in the ion signal. Ground state "flux enhancement" [13] can occur when the scanning laser excites collision pairs at very long range, which then radiatively decay back to the ground state after traveling some distance on an attractive potential, thereby increasing the supply of collision pairs at short range. In contrast, "shielding" [14] occurs when the scanning laser promotes collision pairs to a repulsive potential at large range, reducing the flux at short range. Both effects depend on the relative detuning of the two lasers from each other and from atomic resonance.

The positions of the largest signals in Fig. 2 correspond to known photoassociation transitions to states $|e2\rangle$. This indicates that they are not due to L_2 interacting with molecules in the intermediate state $|e1\rangle$. The states involved here are the $^3\Sigma_g^+$ $(0_g^-)(S + P_{1/2})$ $v = 125$ [15], $J = 2$ and the $A\,^1\Sigma_u^+(0_u^+)$ $v = 159$, $J = 1, 3$ levels. (v is the vibrational quantum number, and J is the rotational quantum number, that is, the mechanical rotation ℓ, plus the total electronic orbital and spin angular momenta; $\mathbf{J} = \ell + \mathbf{S} + \mathbf{L}$.) The shielding mechanism is ruled out because the detuning of L_2 is to the red of any repulsive potential. The flux enhancement mechanism alone cannot account for the dispersive line shape.

These resonances can be understood as Feshbach resonances when the levels are viewed in a field-dressed picture (see Fig. 1b). The near-zero energy scattering states $|E, n_2\rangle$, with energy E and dressed by n_2 photons of laser 2, are nearly degenerate with the excited state $|e2, n_2 - 1\rangle$, dressed with one less photon. The resonance position is tuned by changing the energy (detuning) of the photons from L_2. As the detuning is scanned from red to blue this state moves down and through zero energy from above, becoming "bound." This causes a rapid change in the scattering wave function which enhances and then suppresses the ion signal. In cases where the scattering length is a well-defined quantity the real part goes first negative, and then positive, in a dispersive manner [9,10]. The connection between the scattering length and the wave function behavior is discussed in Ref. [16].

Alternatively, one can view the dispersive structure as resulting from the interference of amplitudes of two quantum-mechanical paths to ionization: (1) the direct photoassociation/ionization path through $|e1\rangle$ and, (2) one in which a pair of atoms is first excited to a molecular state $|e2\rangle$, stimulated back down to an atom-pair ground state, and then photoassociated and ionized through $|e1\rangle$. The phase picked up on path (2) is determined by the detuning from the resonant photoassociation frequency and this path can interfere constructively or destructively with path (1). This situation is related to the Fano configuration-interaction picture used to describe the autoionization of a bound state [17]. In the present case the bound state ($|e2\rangle$) is embedded (in the dressed picture) in the collision continuum. This continuum is coupled to the bound state $|e1\rangle$ by L_1. The most general case would include a coupling between $|e1\rangle$ and $|e2\rangle$, but in our case this coupling is dipole forbidden in first order. When photoassociation spectroscopy is used as a probe of a magnetic Feshbach resonance [2,18] this coupling between $|e1\rangle$ and $|e2\rangle$ must also be considered. Dispersive line shapes would have been difficult to see in those experiments because of the lack of a background signal.

Our apparatus has been described previously [19], and consists of a Zeeman-cooled atomic beam continuously loaded into a MOT. The MOT lasers are switched on and off with a 50% duty cycle, at a 5 KHz rate. Lasers L_1, L_2, and L_{ion} are introduced simultaneously during the periods when the trap lasers are off in order to eliminate any interference from the trapping lasers. The state $|e1\rangle$ is the $v = 123$ [15], $J = 2$ level of the 0_g^- $(S + P_{1/2})$ potential (Condon point $\approx 60a_0$; $1a_0 = 0.0529$ nm). L_{ion} connects this state to an autoionizing doubly excited state of 0_u^- symmetry a few GHz below the $P_{3/2} + P_{3/2}$ asymptote [20]. Excitation out of state $|e1\rangle$ is a resonant process; no ions are produced if either laser L_1 or L_{ion} is not on. The polarizations of the lasers are linear and such that L_1 and L_2 are parallel, and orthogonal to L_{ion}. The resonances in Fig. 2 have Condon points at $\approx 83a_0$ for $v = 159$ of the A state, and $\approx 64a_0$ for $v = 125$ of the 0_g^- state. We have observed similar resonances with Condon points $\approx 40a_0$, inside the Condon point for L_1.

Fluorescence is collected during the trap-on periods and used to monitor atom loss from the trap. The trap loss signals shown are displaced from the true transition positions because the scan speed of the laser is faster than the trap equilibration time. They are shown simply to indicate relative trap loss sizes. In separate scans we have tuned an additional laser to ionize these states directly and obtained

the true positions and line shapes of the photoassociation transitions (see Fig. 3).

The relative symmetries of states $|e1\rangle$ and $|e2\rangle$ are important in order for the states to couple efficiently through the ground state colliding atom pairs. In an $\Omega = 0$ state there is a connection between J and ℓ. The 0_g^- state has the odd (even) J's formed from combinations of the odd (even) partial waves. For the 0_u^+ state it is the odd J lines that have even ℓ. Collisional states of good ℓ connect only to excited states that contain contributions from the same value of ℓ. Hence, in Fig. 2, where $|e1\rangle$ is an even-J line of the 0_g^- state, one can detect changes to the s and d ground state partial waves, which occur when laser L_2 scans over even J's of a 0_g^- state or odd J's of a 0_u^+ state. Since g/u is not a good symmetry in the atomic ground state continuum, resonances from PA transitions to both g and u states are observed when monitoring on a PA transition to a g state.

The coupling to state $|e2\rangle$ is a function of intensity and detuning. Figure 3 shows how the 0_g^- $v = 125$, $J = 2$ Feshbach resonance grows, broadens, and shifts with power. To model these resonances we adapt the optical Feshbach resonance theory in [9], which modifies standard Feshbach resonance theory [17] to include spontaneous emission from $|e2\rangle$. We modify the wave function given there to normalize the incoming flux, a change which significantly affects our expression for the line shape and their expression for the scattering length. We write the wave function as

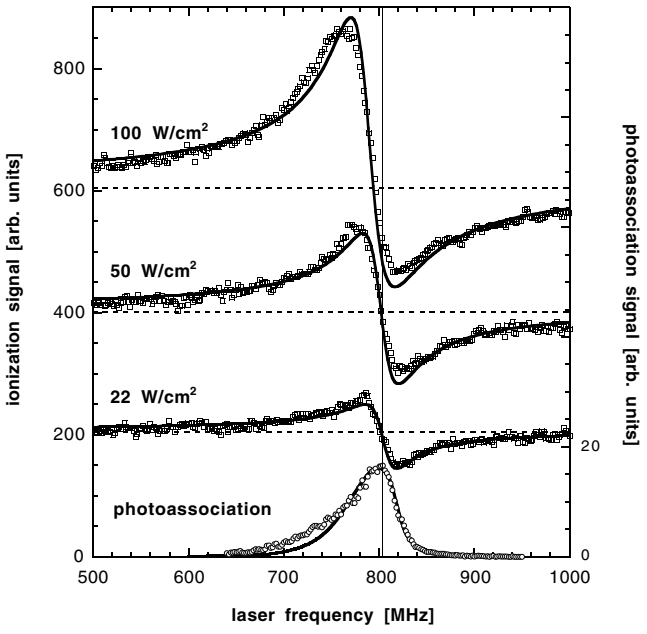

FIG. 3. Variation of the resonance with scanning laser power. The top two traces are offset vertically by 400 and 200 units, respectively. Solid curves through the points are fits to Eq. (2). The dashed lines show the fitted baseline levels. The bottom trace is the low-power photoassociation signal recorded by removing L_1 and tuning L_{ion} to ionize this 0_g^- $v = 125$, $J = 2$ level.

$$\phi(r) = \frac{\Delta + i\frac{\gamma}{2}}{\Delta + i(\frac{\Gamma+\gamma}{2})}\left[\phi_0(r) - \frac{\frac{\Gamma}{2}}{\Delta + i\frac{\gamma}{2}}\phi_1(r)\right], \quad (1)$$

where $\Delta = f - f_0 - \zeta I$, f is the frequency of laser 2, f_0 the natural resonance position, and ζI is the light shift, linear in the intensity I of L_2. γ is the natural linewidth, and Γ is the laser-induced, stimulated absorption/emission rate (also linear in intensity). $\phi_0(r) \to \sin(kr - \frac{\ell\pi}{2} + \theta)$ as $r \to \infty$ is the regular wave function solution to the Schrödinger equation in the absence of light, and $\phi_1(r)$ becomes the irregular solution $[\cos(kr - \frac{\ell\pi}{2} + \theta)]$ at large r. Equation (1) leads to the form for the scattering length given in [10].

The ionization signal $S(\Delta)$ is proportional to a small photoassociation signal from L_1. This signal is proportional to the squared modulus of the overlap between $|e1\rangle$ and the scattering wave function given in Eq. (1):

$$S(\Delta) = A\,\frac{(\Delta - B\frac{\Gamma}{2})^2 + (\frac{\gamma}{2})^2}{\Delta^2 + (\frac{\Gamma+\gamma}{2})^2}, \quad (2)$$

where A is the signal far from the resonance. B is the relative overlap of $|e1\rangle$ with ϕ_0 and ϕ_1. In the limit of zero natural linewidth this reduces to a Beutler-Fano line shape function [17]. Equation (2) can be written as a baseline plus a Lorentzian, plus a dispersion function. This simple form gives a good fit to the resonances as shown in Fig. 3 provided we use a natural linewidth $\gamma = 30$ MHz, somewhat larger than the 20 MHz radiative linewidth. A more complete treatment would include hyperfine structure and thermal averaging. In the present case the monitor laser is tuned to the peak of the photoassociation line and thus only interacts with the velocity subclass that contributes to this portion of the line shape. Therefore we expect the Feshbach signal to have a narrower linewidth than the $\approx$60 MHz FWHM of the photoassociation line shown. Similarly, a more complete treatment would take into account the collisional energy dependence of Γ due to the "Wigner threshold law" scaling of the wave function overlap at low energy (see Fig. 3 of [21]). Our extracted value of Γ is an average over the collision energies monitored.

The fitted resonance position and linewidths shift linearly with power, as expected. Using $B = 3.0$ we find that $\Gamma/I = 0.15$ MHz/(W/cm^2) and the shift parameter $\zeta = 0.22$ MHz/(W/cm^2), assuming a spot size of 0.001 cm^2.

The PA line shown at the bottom of Fig. 3 fits [22] reasonably well to a thermally averaged line shape with contributions from both s- and d-wave scattering, using $\gamma = 23$ MHz and the same $\Gamma = 3$ MHz as for the Feshbach signal. The monitor laser L_1 is tuned to the peak of a PA line and selects out the velocity class of atoms that contributes to the signal at this detuning. Thus, for low laser power, $\Delta = 0$ for the Feshbach line occurs at the same frequency as the peak of the photoassociation line. In a BEC the narrow thermal distribution will

ensure that photoassociation losses will occur only over a frequency range determined by the natural linewidth and that both L_2 and L_1 will interact with all of the atoms present.

A large enhancement of the ionization signal is accompanied in some cases by a relatively large trap loss signal (up to 30% for the $A^1\Sigma_u^+$, $J = 1$ state shown in Fig. 2). In these cases the reduction in the ionization signal near the trap loss resonance is partly accounted for by the reduction in the number of atoms in the MOT. We have not normalized the signals shown in Figs. 2 and 3 to the fluoresence to correct for trap loss effects. For the 0_g^- states the trap loss is sufficiently small (5% or less) that such a normalization does not affect the fits in Fig. 3. Fits to the A-state $J = 1$ line are less satisfactory presumably because of the large trap loss, but simply normalizing the ion signal to trap fluorescence does not improve the fit.

In order to make Feshbach resonances useful for manipulating the scattering length in a BEC one must be able to change the elastic cross section without inducing large losses. Such losses near a number of magnetic Feshbach resonances are severe [1,23]. As can be seen in Fig. 3, a way to avoid the spontaneous emission losses inherent in optical Feshbach resonances is by detuning from the resonance and increasing the intensity, as investigated in detail in Ref. [10]. The deviation of $S(\Delta)$ from its background falls off as Δ^{-1} while the photoassociation signal (loss) falls off approximately as Δ^{-2}. Another method of reducing losses is by using an off-resonant Raman transition [24] to tune a bound ground state through zero energy. Using a bound state with a small decay rate rather than an excited state with a large linewidth should minimize the losses.

There are several potential advantages of optically induced Feshbach resonances over their magnetically induced counterparts. While magnetic Feshbach resonances have already proven to be valuable in manipulating Bose condensates, they are not always easy to implement in the laboratory and put constraints on the traps used to study them. This is particularly true for Na, where the field strengths required are quite large ($\approx$0.1 T). Optically induced Feshbach resonances are ubiquitous and can be applied in optical, static magnetic, or time-orbiting potential traps. Some technical advantages are that the fields can be switched much more quickly; they do not have to be swept through the resonance to reach the "far" side, and both the intensity and detuning are available as control parameters. On the other hand, the need to be substantially detuned from the resonance may limit the range of scattering lengths that can be obtained with reasonable laser powers.

Since an optical field can be easily focused, the field can be nonuniform across the condensate. For instance, half of the condensate can be made to have one scattering length and half another. Pulses of light can create periods of altered scattering length in a condensate, which will lead to excitations. A variety of experiments with time and spatially dependent scattering properties remains to be explored. Finally, one might think of using such optical Feshbach resonances to perform a type of coherent control. Such resonances present an opportunity for changing reaction rates (ionization rates in the present experiment) in a MOT or other environment, in a controlled manner, using an auxiliary field.

We would like to thank Paul Julienne, Carl Williams, Andrea Simoni, Eite Tiesinga, and Fred Mies for identifying this as a Feshbach resonance and for many useful discussions. This work was supported in part by the U.S. Office of Naval Research.

[1] S. Inouye *et al.,* Nature (London) **392**, 151 (1998).
[2] P. Courteille *et al.,* Phys. Rev. Lett. **81**, 69 (1998).
[3] J. Roberts *et al.,* Phys. Rev. Lett. **81**, 5109 (1998).
[4] V. Vuletic, C. Chin, A. Kerman, and S. Chu, Phys. Rev. Lett. **83**, 943 (1999).
[5] V. Vuletic, A. Kerman, C. Chin, and S. Chu, Phys. Rev. Lett. **82**, 1406 (1999).
[6] S. Cornish *et al.,* Phys. Rev. Lett. **85**, 1795 (2000).
[7] A. J. Moerdijk, B. J. Verhaar, and T. M. Nagtegaal, Phys. Rev. A **53**, 4343 (1996).
[8] M. Marinescu and L. You, Phys. Rev. Lett. **81**, 4596 (1998).
[9] P. O. Fedichev, Y. Kagan, G. V. Shlyapnikov, and J. T. M. Walraven, Phys. Rev. Lett. **77**, 2913 (1996).
[10] J. Bohn and P. Julienne, Phys. Rev. A **56**, 1486 (1997).
[11] F. H. Mies, E. Tiesinga, and P. S. Julienne, Phys. Rev. A **61**, 022721 (2000).
[12] K. M. Jones, S. Maleki, L. Ratliff, and P. Lett, J. Phys. B **30**, 289 (1997).
[13] S. D. Gensemer and P. L. Gould, Phys. Rev. Lett. **80**, 936 (1998); C. Orzel, S. Bergeson, S. Kulin, and S. L. Rolston, Phys. Rev. Lett. **80**, 5093 (1998).
[14] L. Marcassa *et al.,* Phys. Rev. Lett. **73**, 1911 (1994).
[15] The vibrational numbering for this state is not known experimentally and is based on *ab initio* calculations.
[16] P. S. Julienne, J. Res. Natl. Inst. Stand. Technol. **101**, 487 (1996).
[17] H. Friedrich, *Theoretical Atomic Physics* (Springer-Verlag, New York, 1990).
[18] F. A. van Abeelen, D. J. Heinzen, and B. J. Verhaar, Phys. Rev. A **57**, R4102 (1998).
[19] L. P. Ratliff *et al.,* J. Chem. Phys. **101**, 2638 (1994).
[20] A. Amelink *et al.,* Phys. Rev. A **61**, 042707 (2000).
[21] J. Bohn and P. Julienne, Phys. Rev. A **60**, 414 (1999).
[22] K. M. Jones *et al.,* Phys. Rev. A **61**, 012501 (2000).
[23] J. Stenger *et al.,* Phys. Rev. Lett. **82**, 2422 (1999).
[24] R. Wynar *et al.,* Science **287**, 1016 (2000).